Physics-Informed Digital Twin with Parameter Refinement for a Field-Trial C+L-Band Transmission Link

Yuchen Song(1), Min Zhang (1), Yan Shi (2), Yu Tang (2), Yakun Hu (2), Shikui Shen, and Danshi Wang (1),*

(1) State Key Laboratory of Information Photonics and Optical Communications, Beijing University of Posts and Telecommunications, Beijing, 100876, China, *danshi_wang@bupt.edu.cn,
(2) China Unicom Research Institute, Beijing, 100044, China.

Abstract *Physics-informed neural operator is learned for multi-channel power evolution and facilitates the parameter refinement for accurate physical layer digital twin, which is demonstrated in a field-trial C+L-band link over different loadings, showing maximum 2.4dB and 1.4dB accuracy improvement for channel power prediction and QoT estimation. ©2023 The Author(s)*

Introduction

Physical-layer digital twin (PHY-DT) attempts to simulate and interact with physical transmission link in real-time and is becoming the cornerstone of the intent-based network control for the intelligent optical networks [1-3]. The accurate estimation of Quality of Transmission (QoT) is crucial for PHY-DT to increase network capacity by exploiting system margin [4] and to facilitate online maintenance throughout the network's lifespan, e.g., amplifier configuration, resource allocation, and fault recovery [5-8]. As the growing data traffic, it is desired to upgrade to C+L-band transmission [9], which brings stronger Kerr nonlinearities and stimulated Raman scattering (SRS) effect, thereby magnifying the complexity and indispensability of PHY-DT.

In contrast to lab experimental testbeds with controlled conditions, field-trial scenarios face severe problems of parameter uncertainties, which necessitates the online parameter refinement for accurate PHY-DT. Particularly, uncertain lump losses before and after each fibre span (i.e., due to lossy splice) will strongly affect the accuracies of the estimation of power and QoT, which have been investigated in [10,11] for C-band transmission. However, when upgrading to L-band, this issue is more intricate due to the disparate lump losses for C and L-band resulting from the separate span amplification. Furthermore, the wider transmission band introduces unneglectable frequency-dependent fibre attenuation and SRS, which has been proved to be important for wideband QoT estimation [12]. The strength of SRS was identified in [13] for various fibres but using time-consuming differential evolution.

The operational speed is critical for PHY-DT. With closed-form perturbation-based nonlinear interference (NLI) estimation [14], the speed bottleneck lies on the computation of fibre channel power evolution, where requires iterative numerical methods to solve a large set of ordinary differential equations (ODEs) [15,16]. Accordingly, a closed-form expression was derived in [17] with sacrificed accuracy. Deep learning-based methods have been proposed for end-to-end modelling in a data-driven manner [16]. However, these methods rely heavily on massive data collection and do not guarantee adherence to underlying physical laws, rendering them unreliable compared to methods based on prior knowledge. To overcome these limitations, recently proposed physics-informed neural networks incorporate physical laws as constraints within the loss function [18,19]. This unique feature makes them well-suited for reliable modelling [20] and parameter identification [21,22].

In this paper, we develop a PHY-DT that utilizes physics-informed modelling techniques for a field-trial C+L-band transmission link. Physics-informed neural operator is learned for channel power evolution in fibre, which improves the calculation speed and ensures compliance with physical laws. In particular, the incorporation of physical laws enables the refinement of lump losses, frequency-dependent attenuation, and SRS strength. Compared to coarse datasheet parameters, the results after refinement yield maximum 2.4dB and 1.4dB improvement for channel power prediction and QoT estimation.

Physics-informed physical layer digital twin

The proposed physics-informed PHY-DT comprises two main modules: fibre and erbium-doped fibre amplifier (EDFA), describing the power evolution along the link and the accumulation of NLI and amplified spontaneous emission (ASE) noise. For NLI power calculation (P_{NLI}), closed-form Gaussian noise (GN) model considering SRS effect is employed [23]. The EDFA model adds ASE noise power (P_{ASE}) and modifies channel power (P_n) with frequency-dependent gain and noise figure profiles. For the multi-channel power evolution in fibre, the governing equation considering frequency-dependent attenuation and SRS is shown below

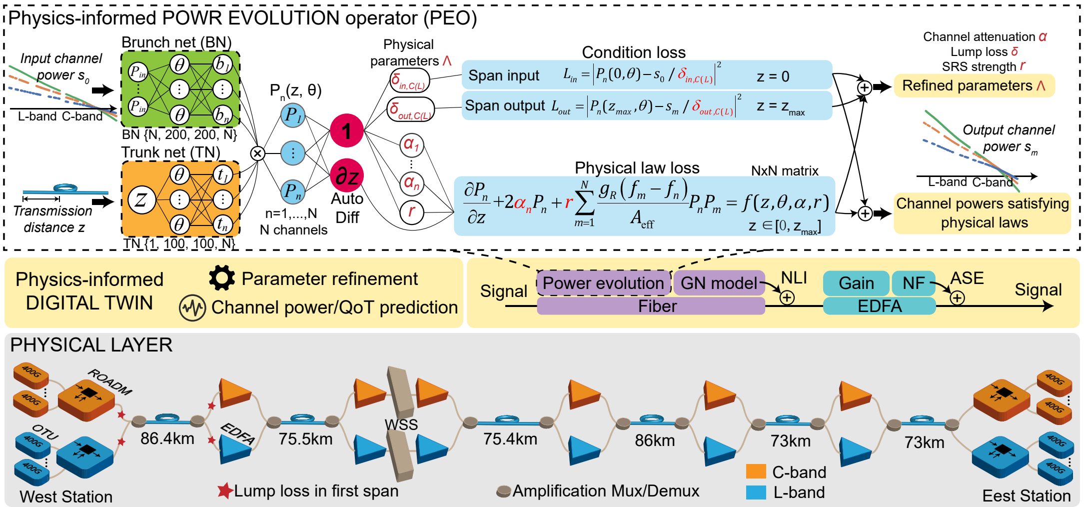

Fig. 1: Schematic of the physics-informed PHY-DT (top) and the field-trial C+L-band transmission link (bottom). OUT denotes optical transport unit. θ denotes parameters of PEO. The number of neurons is shown at the bottom of networks.

$$\frac{\partial P_n(z)}{\partial z} + 2\alpha_n P_n(z) + r\sum_{m=1}^{N} \frac{g_R(f_m - f_n)}{A_{\mathrm{eff}}} P_n(z) P_m(z) = 0\ , \quad (1)$$

being N the number of transmitted channels, α_n the frequency-dependent attenuation, A_{eff} the fibre effective area and f_n the frequency of the nth channel. g_R is the fiber Raman gain spectrum with r being its strength, which is directly related to the power transfer of SRS. For the nth channel, the general signal to noise ratio (GSNR) is used as the QoT metric:

$$GSNR_n = \frac{P_n}{P_{ASE,n} + P_{NLI,n}}\ . \quad (2)$$

For calculation of channel power P_n in fibre, Eq. (1) is typically solved using numerical split-step methods. These methods are computationally expensive with small step size over long transmission, resulting in the increased calculation time of the PHY-DT. In this study, we learn Eq. (1) using a closed-form neural operator in a physics-informed way, as illustrated in the top of Fig. 1. Notably, unlike data-driven neural networks that rely on massive labelled data collection, physics-informed neural operator incorporates the underlying physics [24], i.e., Eq. (1) describing power evolution, as a constraint in the loss function **without any labelled data**. This incorporation of physical laws not only enhances the generalization ability of the learned power evolution operator (PEO) but also enables the refinement of parameters within Eq. (1).

As shown in the top of Fig. 1, the structure of deep neural operator (DeepONet) comprises two neural networks: the branch net (BN) and the trunk net (TN) [25]. The TN samples the transmission distance z as inputs while the BN takes input channel powers s_0 of different loadings as input. The PEO outputs at given z, denoted as $P_n(z, \theta)$, are obtained by merging two net outputs by a vector product. s_0 is learned through the condition loss at z=0. For the physics-informed regularization of PEO, $f(z, \theta, \alpha, r)$ is minimized at random z as depicted in Fig. 1. For each span, the collection of physical parameters to be refined is denoted as $\Lambda = \{\alpha_n, r, \delta_{in,C(L)}, \delta_{out,C(L)}\}$ with the last two being the lump losses at the input and output for C(L)-band. When Λ are known, only the PEO parameter θ is updated, enabling the derivation of $P_n(z, \theta)$ satisfying Eq. (1) and s_0. It should be emphasized that the physical regularization of $P_n(z, \theta)$ requires no labelled data, and the differential term in f can be calculated efficiently using the automatic differentiation built in deep learning libraries.

Physics-informed methods are well-suited for parameter refinement tasks due to their inherent incorporation of physical parameters. The PEO is able for the refinement of Λ with the knowledge of span output channel power s_m measured by optical channel monitoring (OCM). A pre-trained PEO is employed as it can provide a suitable starting point. Λ are updated along with the network parameters θ, ensuring the satisfaction of the constraints f and the boundary conditions at z=0 and z=z_{max} as illustrated in Fig. 1.

Field-trial C+L-band transmission link

The field-trial C48+L48 WDM transmission link under analysis in China Unicom's metro optical networks is illustrated in Fig. 1. It consists of six amplified spans with a maximum length of 86.4km (totalling 469.3km of G.652 SMF). A dynamic gain equalizer (DGE) is placed at the second site for channel power equalization, while in other sites, in-line EDFA is deployed for separated amplification of C- and L-band. OCM is placed at the front and end of EDFA for channel power collection. Three commercial 400Gb/s transponders on the C-band and two on the L-band are configured for five channels under test (CUT), and PCS-16QAM with 91.6 baud rate is

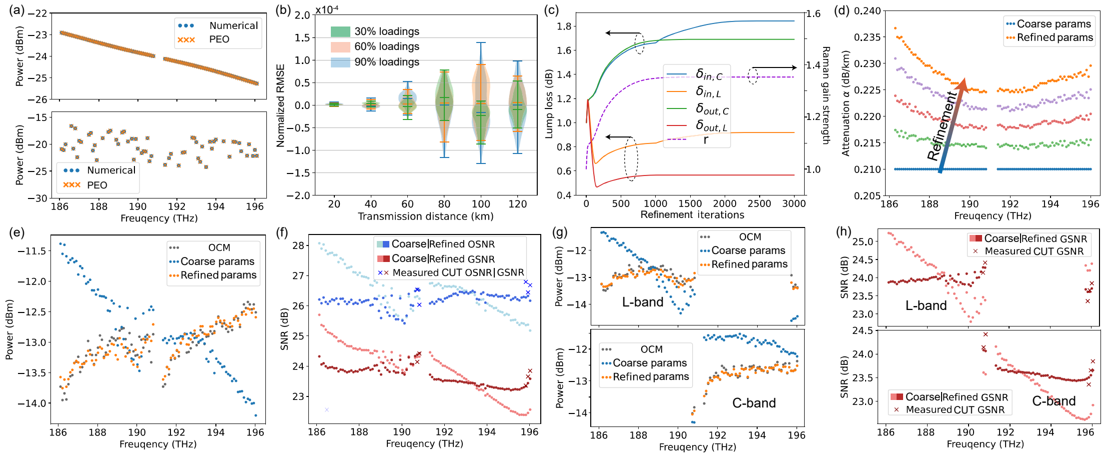

Fig. 2: (a) Channel powers at 120km for two loadings. (b) Statistical testing results for PEO under different loadings and distances. (c)(d) Update of refined parameters. Estimation of channel powers (e)(g) and QoT (f)(h) for three loads with refined parameters.

modulated for optical transmission with 100GHz channel spacing. In the transceiver side, signals are mux/demux by ROADM, and other channels are filled with filtered ASE noise for full loading on C+L-band. The transmission bandwidth occupies the L-band, from 186.1 THz to 190.8 THz, and the C-band, from 191.4 THz to 196.1 THz with a total of 96 channels. We focus on the transmission from west to east station in this paper. The state of the network, including channel powers and EDFA config, was obtained by querying via controller. The link has been configured to an optimal performance by a vendor controller.

Simulations for real-time forward prediction

First, we select 5,000 different s_0 at z=0 with random loadings to train this PEO, and for each channel, the launch power was either 0mW or varied between 0.1mW to 8mW. The transmission distance is sampled from 0 to 120km. Approximately 1 hour was paid in the training process with GPU Tesla T4. However, once trained, the PEO can generalize well to unseen s_0 thanks to the guidance of physical laws. Fig. 2(a) reports testing results after 120km transmission, with one full loading of uniform 1mW launch power and a case of 80% random loading. Both results agree well with the numerical split-step methods of 100m step size, and the statistical test results are displayed in Fig. 2(b). For testing cases with 1,000 new random loadings and within 120km, the normalized root mean-square-error (RMSE) generally falls in 1x10^{-4}. It can be observed that the accuracy decreases a bit with longer distance and more channels. The time can be reduced by up to 100 times using the closed-form PEO compared to numerical methods in this set up (network size is shown in Fig. 1). The PEO serves as a fast yet accurate solver for channel power prediction.

Field-trial validations of PHY-DT

We take the first span of this operating field-trial link as an example, the coarse data-sheet parameters of Λ are $\delta_{in(out),C(L)}$=1dB, α=0.21dB/km, and r=1. Eight pairs of channel powers before and after this span measured by OCM along the regular operations are used as boundary conditions. The updating trace of these refined parameters are depicted in Fig. 2(c)(d). This process can be done parallelly for each span. With these refined parameters, the prediction accuracy for channel power and QoT can be improved. The results for full loading are shown in Fig. 2(e)(f), and the accuracy of power is improved from 1.1 to 0.12 (RMSE in dB units) with a per-channel accuracy improvement of 0.8dB in average and 2.4dB in max. For CUT, the measured OSNR are delivered from controller, and the GSNR is derived from pre-FEC BER. The maximum per channel accuracy improvement of OSNR and GSNR for CUT is 1.6 and 1.4dB, respectively. For partial loading of C- and L-band, where the ASE channels are removed, the accuracy is overall improved as shown in Fig. 2 (g)(h). It is worth noting that our approach remains effective even without OCM at the front of EDFA. In such cases, the non-flat gain profile can be absorbed in the refined parameters.

Conclusions

The effectiveness of physics-informed PHY-DT has been demonstrated on a field-trial C+L-band transmission link. The physics-informed PEO significantly reduces the operation time of PHY-DT without compromising accuracy and enables online parameter refinement, resulting in a QoT estimation error reduction of up to 1.4dB across different loadings. This paper paves the way for the use of hybrid data and physics-based methods for PHY-DT in optical networks.

Acknowledgements

National Natural Science Foundation of China (No. 62171053, 61975020) and BUPT Excellent Ph.D. Students Foundation (No. CX2022123).

References

[1] G. Borraccini, S. Straullu, A. Giorgetti, R. Ambrosone, E. Virgillito, A. D'Amico, R. D'Ingillo, F. Aquilino, A. Nespola, and N. Sambo, "Experimental Demonstration of Partially Disaggregated Optical Network Control Using the Physical Layer Digital Twin," arXiv preprint, DOI: 10.48550/arXiv.2212.11874.

[2] Q. Zhuge, "AI-driven Digital Twin for Optical Networks," in European Conference and Exhibition on Optical Communication, 2022: Optica Publishing Group, p. Mo3A. 1.

[3] D. Wang, Z. Zhang, M. Zhang, M. Fu, J. Li, S. Cai, C. Zhang, and X. Chen, "The role of digital twin in optical communication: fault management, hardware configuration, and transmission simulation," IEEE Communications Magazine, vol. 59, no. 1, pp. 133-139, 2021, DOI: 10.1109/MCOM.001.2000727.

[4] A. W. MacKay and D. W. Boertjes, "Field Learnings of Deploying Model Assisted Network Feedback Systems," in Optical Fiber Communication Conference, 2022: Optica Publishing Group, p. W4G. 2, DOI: 10.1364/ofc.2022.w4g.2.

[5] B. Correia, R. Sadeghi, E. Virgillito, A. Napoli, N. Costa, J. Pedro, and V. Curri, "Power control strategies and network performance assessment for C+L+S multiband optical transport," Journal of Optical Communications and Networking, vol. 13, no. 7, p. 147, 2021, DOI: 10.1364/jocn.419293.

[6] N. Sambo, A. Ferrari, A. Napoli, N. Costa, J. Pedro, B. Sommerkorn-Krombholz, P. Castoldi, and V. Curri, "Provisioning in Multi-Band Optical Networks," Journal of Lightwave Technology, vol. 38, no. 9, pp. 2598-2605, 2020, DOI: 10.1109/jlt.2020.2983227.

[7] Y. Song, Q. Fan, C. Lu, D. Wang, and A. P. T. Lau, "Efficient Three-Step Amplifier Configuration Algorithm for Dynamic C+ l-Band Links in Presence of Stimulated Raman Scattering," Journal of Lightwave Technology, 2022, DOI: 10.1109/jlt.2022.3223919 .

[8] M. Devigili, M. Ruiz, N. Costa, A. Napoli, J. Pedro, and L. Velasco, "Dual Time and Frequency Domain Optical Layer Digital Twin," in European Conference and Exhibition on Optical Communication, 2022, p. Tu5. 42.

[9] M. Cantono, R. Schmogrow, M. Newland, V. Vusirikala, and T. Hofmeister, "Opportunities and Challenges of C+L Transmission Systems," Journal of Lightwave Technology, vol. 38, no. 5, pp. 1050-1060, 2020, DOI: 10.1016/b978-0-12-374965-9.10003-2.

[10] A. Ferrari, K. Balasubramanian, M. Filer, Y. Yin, E. Le Rouzic, J. Kundrát, G. Grammel, G. Galimberti, and V. Curri, "Assessment on the in-field lightpath QoT computation including connector loss uncertainties," Journal of Optical Communications and Networking, vol. 13, no. 2, p. A156, 2020, DOI: 10.1364/jocn.402969.

[11] N. Morette, I. F. de Jauregui Ruiz, H. Hafermann, and Y. Pointurier, "On the robustness of a ML-based method for QoT tool parameter refinement in partially loaded networks," in Optical Fiber Communication conference, 2022: Optica Publishing Group, p. M3F. 1, DOI: 10.1364/ofc.2022.m3f.1

[12] A. D'Amico, B. Correia, E. London, E. Virgillito, G. Borraccini, A. Napoli, and V. Curri, "Scalable and Disaggregated GGN Approximation Applied to a C+L+S Optical Network," Journal of Lightwave Technology, pp. 1-1, 2022, DOI: 10.1109/jlt.2022.3162134.

[13] U. C. de Moura, D. Zibar, A. Margareth Rosa Brusin, A. Carena, and F. Da Ros, "Fiber-Agnostic Machine Learning-Based Raman Amplifier Models," Journal of Lightwave Technology, vol. 41, no. 1, pp. 83-95, 2023, DOI: 10.1109/jlt.2022.3210769 .

[14] P. Poggiolini, "The GN Model of Non-Linear Propagation in Uncompensated Coherent Optical Systems," Journal of Lightwave Technology, vol. 30, no. 24, pp. 3857-3879, 2012, doi: 10.1109/jlt.2012.2217729, DOI: 10.1109/jlt.2012.2217729 .

[15] I. Roberts, J. M. Kahn, J. Harley, and D. W. Boertjes, "Channel Power Optimization of WDM Systems Following Gaussian Noise Nonlinearity Model in Presence of Stimulated Raman Scattering," Journal of Lightwave Technology, vol. 35, no. 23, pp. 5237-5249, 2017, doi: 10.1109/jlt.2017.2771719, DOI: 10.1109/jlt.2017.2771719.

[16] A. R. Brusin, M. R. Zefreh, P. Poggiolini, S. Piciaccia, F. Forghieri, and A. Carena, "Machine learning for power profiles prediction in presence of inter-channel stimulated Raman scattering," in 2021 European Conference on Optical Communication (ECOC), 2021: IEEE, pp. 1-4, DOI: 10.1109/ecoc52684.2021.9605807.

[17] A. Anchal and E. Lichtman, "A Few Milliseconds-Fast SRS-Induced Loss and Tilt Compensation Algorithm for Dynamic C+ L-band Networks," in European Conference on Optical Communication (ECOC), 2022, pp. 1-4.

[18] M. Raissi, P. Perdikaris, and G. E. Karniadakis, "Physics-informed neural networks: A deep learning framework for solving forward and inverse problems involving nonlinear partial differential equations," Journal of Computational Physics, vol. 378, pp. 686-707, 2019, DOI: 10.1016/j.jcp.2018.10.045.

[19] D. Wang, X. Jiang, Y. Song, M. Fu, Z. Zhang, X. Chen, and M. Zhang, "Applications of physics-informed neural network for optical fiber communications," IEEE Communications Magazine, vol. 60, no. 9, pp. 32-37, 2022, DOI: 10.1109/mcom.001.2100961.

[20] Y. Song, D. Wang, Q. Fan, X. Jiang, X. Luo, and M. Zhang, "Physics-Informed Neural Operator for Fast and Scalable Optical Fiber Channel Modelling in Multi-Span Transmission," in 2022 European Conference on Optical Communication (ECOC), 2022, pp. We.32.

[21] Y. Song, Y. Zhang, C. Zhang, J. Li, M. Zhang, and D. Wang, "PINN for Power Evolution Prediction and Raman Gain Spectrum Identification in C+ L-Band Transmission System," in Optical Fiber Communication Conference, 2023, p. Th1F. 5.

[22] X. Jiang, D. Wang, X. Chen, and M. Zhang, "Physics-Informed Neural Network for Optical Fiber Parameter Estimation From the Nonlinear Schrödinger Equation," Journal of Lightwave Technology, vol. 40, no. 21, pp. 7095-7105, 2022, DOI: 10.1109/jlt.2022.3199782.

[23] D. Semrau, E. Sillekens, R. I. Killey, and P. Bayvel, "A Modulation Format Correction Formula for the Gaussian Noise Model in the Presence of Inter-Channel Stimulated Raman Scattering," Journal of Lightwave Technology, vol. 37, no. 19, pp. 5122-5131, 2019, DOI: 10.1109/jlt.2019.2929461.

[24] S. Wang, H. Wang, and P. Perdikaris, "Learning the solution operator of parametric partial differential equations with physics-informed deeponets," Science advances, vol. 7, no. 40, p. eabi8605, 2021, DOI: 10.26226/morressier.612f6736bc98103724100850.

[25] L. Lu, P. Jin, G. Pang, Z. Zhang, and G. E. Karniadakis, "Learning nonlinear operators via DeepONet based on the universal approximation theorem of operators," Nature Machine Intelligence, vol. 3, no. 3, pp. 218-229, 2021, DOI: 10.1038/s42256-021-00302-5.